Supplementary Information (SI) for Green Chemistry.
This journal is © The Royal Society of Chemistry 2024

A facile methodology for side- and up- cycling of HDPE waste via partial creation of unsaturated double bonds

Wenyu Wu Klingler *[a], Lucie Perret [a], Patrick Rupper [a], Sandro Lehner [a], Xiaoyu Zhou [b], Henrik Eliasson [c], Rico Muff [d], Manfred Heuberger [a, e], Sabyasachi Gaan [a]

a Laboratory for Advanced Fibers, Empa, Swiss Federal Laboratories for Materials Science and Technology, Lerchenfeldstrasse 5, 9014 St. Gallen, Switzerland

b Department of Chemistry and Applied Biosciences, ETH Zürich, Vladimir Prelog Weg 1–5, 8093 Zürich Switzerland

c Electron Microscopy Center, Empa, Swiss Federal Laboratories for Materials Science and Technology, Überlandstrasse 129, 8600 Dübendorf, Switzerland

d Transport at Nanoscale Interfaces Laboratory, Empa, Swiss Federal Laboratories for Materials Science and Technology, Überlandstrasse 129, 8600 Dübendorf, Switzerland

e Department of Materials, ETH Zurich, 8092 Zurich, Switzerland

Table of content

Experimental details

Material and General Methods

All operations involving air sensitive reagents and materials during catalysts precursor synthesis and activation were carried out under nitrogen atmosphere using standard Schlenk and dry box techniques. High-density polyethylene named by supplier Exxon Mobil (Saudi Arabia) as ExxonMobil HDPE HMA 018 (HDPE) was specified by melt flow rate (MFR) equal to 30 g/10 min (according to ASTM D 1238, 190 °C/2.16 kg), with density around 0.954 g/cm^3. Nitric acid (70%), anhydrous toluene (99.8%), Chloroform (99.2%), 1,5-pentanediol, titanium(IV) butoxide, and 1 wt% Pt on alumina pellets (3.2 mm) were purchased from Sigma-Aldrich. All chemicals were used as received without further purification.

Characterizations

Gel permeation chromatography (GPC) analyzes were carried out on the samples. Around 2-4 mg of material were dissolved in 1 mL of 1,2,4-trichlorobenzene (TCB) containing 0.0125 % dibutylhydroxytoluene (BHT). The solution was let pass through a 1260 Infinity II High Temperature GPC System (Agilent Technologies, USA) equipped with a triple detector (refractive index detector, viscometer and light scattering detector). Measurements were performed with two Agilent PLgel Olexis (13 µm particle size) columns (Agilent Technologies, USA) in series, after calibration with PS standards. The measurement conditions that were chosen are the following: column temperature of 160 °C, flow of 1 mL/min of TCB containing 0.0125% BHT as the solvent, and injection volume of 100 µL.

Thermogravimetric analysis (TGA) was performed with a TGA 209 F1 Iris (Netzsch) instrument under N_2 atmosphere and air (unless mentioned) with a heating rate of 10 °C min^{-1}. The melting points were determined by the **differential scanning calorimeter** (**DSC**, 214-Polyma).

^{1}H, ^{13}C and ^{31} P **Nuclear Magnetic Resonance (NMR)** spectra were recorded on a Bruker AV-III 400 spectrometer (Bruker BioSpin AG, Switzerland) using a 5 mm CryoProbe™ Prodigy probe at 400.2, 100.6 and 162.0 MHz, respectively. All NMR experiments were performed at 298 K using the Bruker standard pulse programs and parameter sets applying 90° pulse lengths of 12.0 µs (^{1}H), 10.5 µs (^{13}C) and 10.7 µs (^{31}P). ^{1}H and ^{13}C NMR chemical shifts (δ) were calibrated to residual solvent peaks.

X-ray diffraction (XRD) patterns were recorded with a Panalytical XPert3Powder instrument, operating at a voltage of 40 kV and a current of 40 mA with Cu/Ka radiation having a wavelength of 1.5406 Å. XRD patterns were recorded over an angular range (2ϑ) of 5–80°. The identification of peaks and patterns was based on American Mineralogist Crystal Structure Database.

N_2 adsorption–desorption analysis was conducted using a BELMini device supplied by BEL Japan Inc. The samples were pretreated at 150 °C under vacuum for 16 hours. Hydrogen uptake isotherms were collected at 298 K under static volumetric conditions with a Micromeritics ASAP 2010 apparatus. The first adsorption isotherm was obtained by measuring the adsorbed amount of hydrogen at hydrogen pressures from 1 to 100 kPa. The total adsorbed amount was obtained by extrapolating the linear high-pressure part of the isotherm to zero pressure. The weakly adsorbed hydrogen was removed by

evacuating for 2 h at the analysis temperature (298 K) and a second isotherm was measured. The amount of strongly adsorbed hydrogen is the difference between the first and second isotherms. The H/M ratio is the ratio of the number of adsorbed hydrogen atoms to the total number of metal atoms.

Attenuated total reflection-Fourier transform infrared (ATR-FTIR) spectra were recorded on a Bruker FT-IR in transmission mode.

Transmission electron microscopy (TEM) was carried out using a TEM/STEM JEOL JEM 2200 FS microscope operating at 200 kV. Additionally, high-angle annular dark-field scanning transmission electron microscopy (HAADF-STEM) images were obtained using a probe-corrected Titan Themis, operated at 300 kV. Prior to preparation of composite dispersion, the catalyst pellet were cryo-milled to get a fine powder. The powder was mixed with methanol (0.5 mg/ml) and applied to a copper TEM grid coated with a lacey carbon film. The methanol was evaporated, and the sample was then plasma-cleaned in an argon-oxygen plasma for 10 s before being inserted into the microscope. The images were analyzed by Image J to determine the particle size and distribution.

Scanning Electron Microscope (SEM) and **energy dispersive X-Ray spectroscopy (EDX)** mapping experiments were conducted on Hitachi S-4800, with Au/Pd (6 nm) coated samples.

Raman spectra were acquired using a WITec Alpha 300 R confocal Raman microscope (Oxford Instrument, WITec GmbH, Ulm, Germany) in backscattering geometry. As an excitation source, a laser with 532 nm wavelength was used. The light was focused onto the sample using a 100× objective with a working distance of 4mm and a numerical aperture of 0.75, resulting in a diffraction-limited in-plane laser spot size of <1 µm. The confocality of the Raman microscope limits the focal depth to approximately < 1 µm. The Rayleigh scattered light was blocked by a notch filter. The backscattered light was coupled to a 300 mm lens-based spectrometer with a grating of 600 g/mm for all samples. The spectrometer is equipped with a thermoelectrically cooled CCD (1600×200 pixel, pixel size 16×16 μm^2) leading to a spectral resolution of < 0.85 cm^{-1}. Raman spectra were acquired with a set laser power of 10 mW and an integration time of 1.0 second for the powder samples.

Ultra performance liquid chromatography - Mass spectrometry (UPLC-MS) was used to evaluate the depolymerized products from oxidation experiments. The water soluble products were diluted in water, filtered and injected in Waters Aquity H-Class UPLC system (C18 column, 1.7 µm, 2.1 * 50 mm) at 40 °C (run time 5 min, flow 0.5 ml/min) with a gradient method (at 0 min 95% water, 5% acetonitrile at 3 min 20% water, 80% acetonitrile, at 3.1 min 95% water, 5% acetonitrile, at 5 min 95% water, 5% acetonitrile). The eluent was analyzed with MS (Qda from Waters), in both ESI +/- modes, cone voltage 20V with a mass range of 80–1250 m/z.

X-ray photoelectron spectroscopy (XPS) measurements were performed using a scanning XPS microprobe spectrometer (PHI Quantum 2000, Physical Electronics) with monochromatic Al Kα radiation (1486.6 eV). A photoemission take-off angle of 45° (with respect to the sample surface) was used. The operating pressure of the XPS analysis chamber was below 1 x 10^{-6} Pa for all data presented here. The powder samples were pressed onto an indium foil (Alfa Aesar, 99.99%, 0.25 mm thick) resulting in a contiguous and flat sample surface. The foil is then mounted onto a stainless steel holder

via screws and a mask. Thereby, no signal from the indium substrate was observed. Survey scan spectra (0 – 1360 eV) were acquired with an energy step size of 0.8 eV, an acquisition time of 240 ms per data point and an analyzer pass energy of 187.85 eV. For the element carbon, also higher resolution region spectra were acquired for C 1s (278 – 298 eV) and C KLL (1200 – 1250 eV). For the photoelectron line, an energy step size of 0.125 eV, acquisition time of 1.92 s per data point and an analyzer pass energy of 29.35 eV were used, whereas the corresponding values for the weaker Auger line were 0.2 eV/step, 0.8 s acquisition time and 93.9 eV pass energy to increase the signal-to-noise ratio. Under these conditions, the energy resolution (FWHM, full width at half maximum height) measured on the silver Ag $3d_{5/2}$ is about 2 eV (survey), 0.7 eV (region photoelectron line) and 1 eV (region Auger line). Total acquisition times were approximately 7 min for survey scans and 10 min together for the two region scans. For each sample, two randomly chosen spots were measured using a micro-focused X-ray beam (100 µm, 25 W at 15 kV). The 180° spherical capacitor energy analyzer was operated in the fixed analyzer transmission (FAT) mode. Sample charging of the polyethylene samples was compensated using dual beam charge neutralization with a flux of low energy-electrons (1 eV) combined with very low energy positive Ar ions (8 eV). More details about the XPS system and measurements have been previously published.[1]

In order to be able to use the binding energy position of the carbon C 1s to determine the sp^2 and sp^3 functionality of the investigated samples, the binding energy scale was calibrated using a cellulose sample (Whatman filter paper, ashless) also present on the holder (same mask mounting on indium foil) and referencing it to the known binding energy of the C 1s C-O signal from cellulose of 286.7 eV. [2] Intensity determination and curve fitting was carried out with CasaXPS software version 2.3.16 (Casa Software Ltd, Teignmouth, UK) using a fixed 70% Gaussian, 30% Lorentzian product function to fit (least-squares) the XPS spectra. Atomic concentrations were calculated from XPS peak areas after subtracting a Shirley type background. Thereby, tabulated PHI sensitivity factors corrected for our system's transmission function and analyzer asymmetry parameter (correction due to a different angle between X-ray source and analyzer) have been used for quantification.[3] Experimental spectra of the Auger C KLL region were smoothed (15 points linear Savitzky – Golay routine) and subsequently differentiated (9 points quadratic Savitzky – Golay routine) in order to determine the *D* parameter (peak-to-peak spectrum width of the main C KLL transition).

Investigating a defined polystyrene - polyethylene copolymeric system with known C sp^2/sp^3 ratios, Turgeon and Paynter have shown that the *D* parameter varies in a systematic manner with the sp^2 concentration and hence, can be used to determine the polymeric carbon sp^2/sp^3 ratio.[4] Their corresponding values of the *D* parameter (13.4 eV and 16.0 eV for 100% C sp^3 and 25% C sp^3, respectively) have been applied in this work to evaluate the content of C sp^2/sp^3 bonds in our samples from a linear calibration line. The successfulness of this procedure was shown in the past by Lesiak and co-workers.[5]

Dehydrogenation of HDPE

The introduction of C=C double bonds into aliphatic polymer chains would offer a starting point for a very diverse manifold of reactivity. Further, a partially unsaturated polyolefin could be cross-linked

with standard techniques to give materials with enhanced mechanical properties.[6] Dehydrogenation of aliphatic polyolefins to give partially unsaturated hydrocarbon is endothermic, therefore the use of catalyst is critical to lower the required energy in this process.[7] Significant progress has been made in the past two decades toward the development of varied metal based catalysts for the dehydrogenation of alkanes. [8-11] Porous matrix[12] loaded platinum showed particularly promising selectivity, durability and stability in this context.[9, 13] Herein, we use heterogeneous catalyst for the dehydrogenation of aliphatic linear polyolefins. In addition, some previous studies showed the selective dehydrogenation for branches vs. backbone, resulted by the kinetic selectivity for the terminal positions.[14] Therefore, high density polyethylene with predominantly linear structure was chosen for this study. Following a procedure as shown in **Fig. S1**, the catalyst was dried and reduced by H_2 at 250 °C for 2 h for next steps. The morphology of the platinum subnano/nanoparticles has been confirmed by mean of TEM and XRD before and after activation. Then they are directly used to dehydrogenate the HDPE.

After obtaining the pulverized HDPE, one drying step was used before further treatment. The dehydrogenation step is a solvent-assisted catalytic reaction, whereby the mechanically pulverized HDPE (1 g) was mixed with 1 wt% catalyst (0.5 g pellet) in 10 mL dry toluene, which is then heated to 250 °C for **36, 48 or 72** hours (**HDPE-36**, **HDPE-48**, and **HDPE-72**) under N_2. After reaction, the polymer was collected and the catalyst was washed with hot toluene (2*5mL, 120 °C). The organic part was collected and dried under rotavap. The HDPE was separated and the solvent was recycled for reuse. The treated HDPEs were further vacuum dried to remove any residual solvent and prepare them for subsequent characterization.

Microwave-Assisted oxidation of treated HDPE

Dicarboxylic acids were produced using microwave-assisted oxidative degradation of the dehydrogenated HDPE. Nitric acid was selected for their ability to oxidatively degrade inert polyolefin into fragments and functional products.[15, 16] The preliminary testing was performed in a Milestone SyntWAVE single reaction chamber microwave (Shelton, CT) for 1 hour at 180 °C with 10 min ramp time, and the pressure was kept constant at 60 bar under N_2 atmosphere for the duration of the reaction. Untreated and treated HDPE (1 g) were placed in a heavy-walled glass vials in 10 mL of 0.10 g/mL aqueous nitric acid solution with Teflon cap. The reaction mixture was continuously stirred with a magnetic stirrer during the irradiation. The power was 1200 W for the duration of the reaction. The reaction temperature, pressure and irradiation power were constantly monitored during the course of the reactions. After cooling down, the treated HDPE was totally depolymerized to soluble fragments, while the untreated HDPE was not totally depolymerized into soluble fragments. Both of the solutions were directly sent for UPLC-MS analysis to determine all the organic species. Then, the solutions were neutralized until pH ~ 4, and the desired products were extracted with chloroform (7 mL * 3). Then the organic solvent was removed and paste was collected by rotary evaporation and the obtained product was dried in a vacuum oven. The isolated long-chain dicarboxylic acids (LCDAs, 0.84 g) was determined by NMR and FTIR. The rest is remaining in the neutralized water phase and neutralized until pH ~ 7 for disposal.

Polycondensation of the isolated LCDA diacids

The poly(pentanediol LCDA) polymer was prepared following the two-step melt polycondensation method as reported for other aliphatic polyesters.[17] In the first stage, the 1,5-pentanediol diol, titanium(IV) butoxide (0.05 mol%), and LCDAs were mixed with temperature increasing to 180 °C, and kept 3 hours until no more water was distilled off under N_2 flow. Some samples was collected for analysis. In the second stage, the temperature was risen to 230 °C, and the pressure was reduced to 0.5 mbar to facilitate the removal of the excess of water. After 3 hours, the reaction was stopped, and the polymer was collected directly for characterization.

Regeneration of the catalyst

After the dehydrogenation step, the catalyst was washed by recycled toluene and collected for regeneration. A calcination step under 500 °C for two hours with temperature ramp of 3 °C/min was used. Then the pellets were reactivated using H_2 at 250 °C for two hours for next steps. The morphology of the platinum nanoparticles has been confirmed by mean of TEM, SEM and EDX.

HDPE conformation change after dehydrogenation

Differential scanning calorimetry (DSC) can also be used to study the degree of crystallinity of HDPE. The degree of crystallinity (X_c) can be calculated by the melting enthalpy:

$$Xc = \frac{\Delta H_{m2}}{\Delta H^0{}_m}$$

where ΔH_{m2} is the measured heat of fusion, $\Delta H^0{}_m$ is the heat of fusion of 100% crystalline HDPE (290 J/g).[18]

In addition, the crystalline fraction can be estimated using the equation based on Raman spectra:

$$Xc = \frac{I_{1416}}{I_{(1295+1300)}} \times \frac{100}{0.46}$$

where I_{1416} is the integrated intensity of the band at 1416 cm^{-1} normalized to that of the CH_2 twisting area of 1295 cm^{-1} and 1305 cm^{-1}, which act as an internal standard. The constant 0.46 was determined in the literature from the corresponding intensity of the 1416 cm^{-1} peak of 100% crystalline polyethylene.[19]

Carbon conversion yield

Carbon conversion yield is calculated using a rough estimation of equally distributed diacids, with an averaged molecular weight of C9, C10, C11, C12, and C13 diacids, which is 216.28 g/mol for a C11 diacid. And for 1 g of HDPE, the carbon is averaged with CH2 groups, therefore the following simplified equation is used for estimation:

$$C\% = 100\% \times \frac{\frac{m_{products}}{216.28} \times 11}{\frac{1.0}{14}}$$

Additional Figures

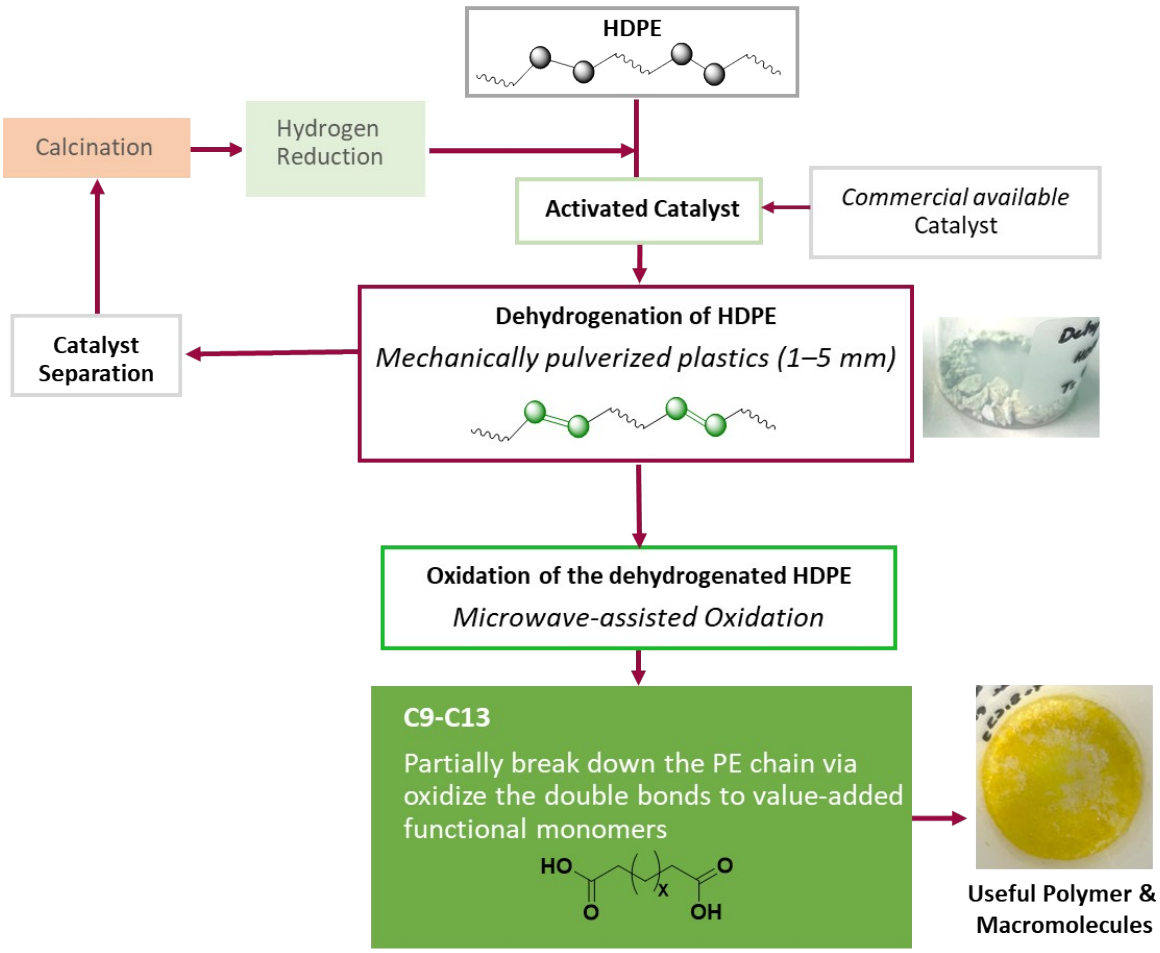

Fig. S1 *Work flow of the two-step depolymerization process, including HDPE dehydrogenation and oxidation.*

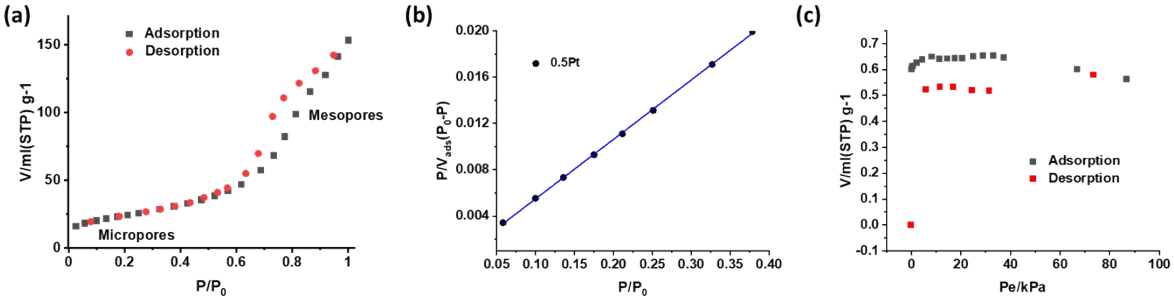

Fig S2*. (a) N_2 adsorption-desorption isotherms, (b) BET curve, and (c) hydrogen uptake isotherms collected at 298 K, of the alumina supported Pt catalysts.*

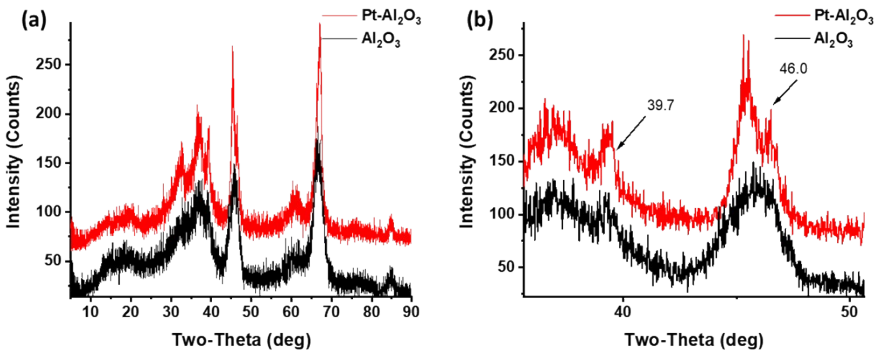

Fig. S3 *XRD patterns of the Pt/Al_2O_3 catalysts and the Al_2O_3 matrix (a).and (b) the partial enlarged area.*

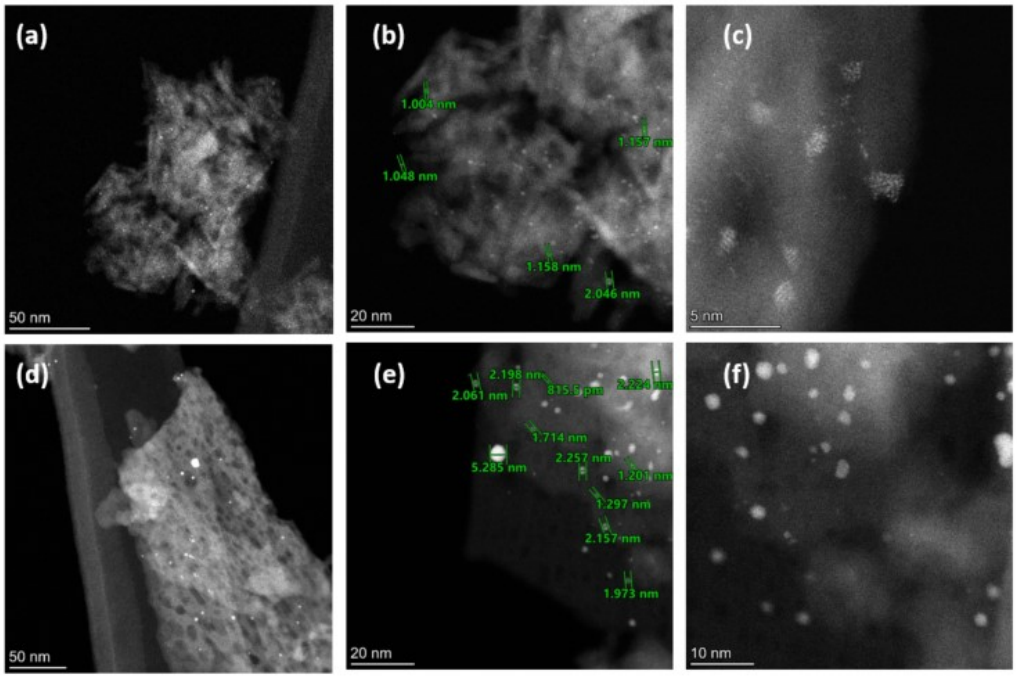

Fig.S4 *STEM micrographs of the before (a, b and c) and after (d, e and f) treated pellet catalyst with annotated size of Pt nanoparticles (middle column).*

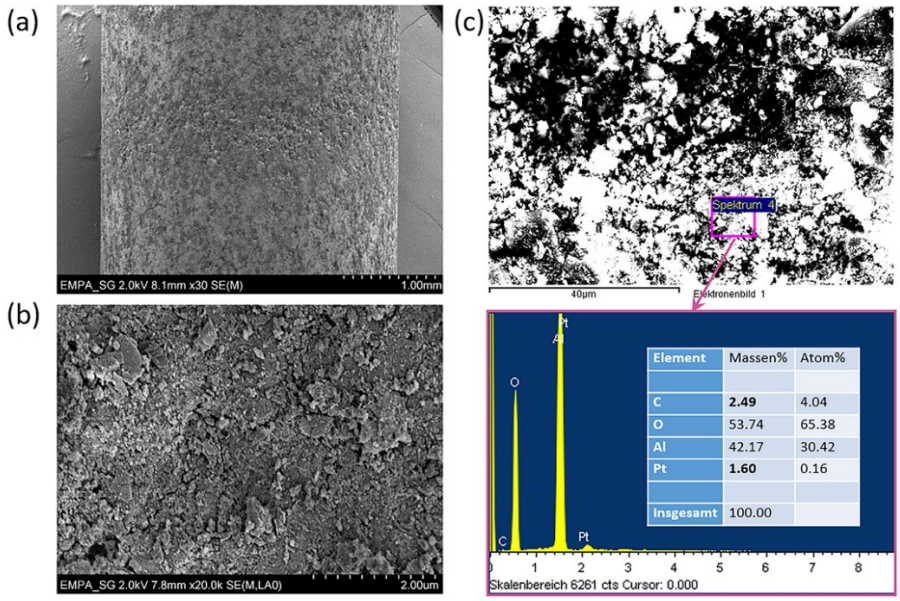

Fig. S5 *SEM and EDX of the catalyst as obtained, (a) and (b) the surface morphology at different scales, and (c) EDX spectrum from a selected range with semi-quantitative amount of the elements.*

Table S1*. Molecular weights determined by GPC analysis of the pristine and treated HDPE at difference conditions, and thermal properties measured by DSC and TGA.*

Samples	M_n (g/mol)	M_w (g/mol)	PD (M_w/M_n)	T_{m1} (°C) *	T_c (°C) *	T_{m2} (°C) *	ΔH_m (J/g)	Xc (%)	$T_{5\%}$ (°C) #	$T_{d.}$ (°C) #
HDPE Blank	13592	49632	3.65	132.0	113.1	132.0	174.8	61.3	426.3	479.4
HDPE-36	13221	52753	3.99	132.1	109.6	129.6	179.9	63.1	441.2	479.4
HDPE-48	13060	50178	3.84	130.8	114.4	129.7	181.2	63.6	437.1	479.5
HDPE-72	15375	55393	3.60	130.7	114.5	129.6	179.5	63.0	441.7	481.2

* T_{m1} measured by the DSC first heating up, T_c measured by cooling, T_{m2}, and enthalpies (ΔH_m) measured by the second heating up, with heating/cooling rate of 10 °C/min.

$T_{5\%}$ is measured at the 5% weight loss point, $T_{d.}$ Is measured at the highest weight loss rate point, using TGA measurement.

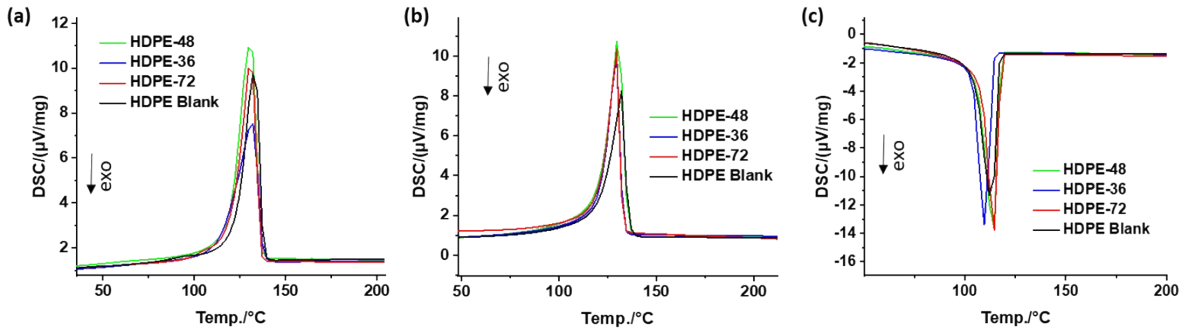

Fig. S6 *DSC curves of untreated and treated HDPE for (a) First melting curve in the DSC measurement, (b) second melting scans, and (c) crystallization measurements at heating rate of 10 °C/min.*

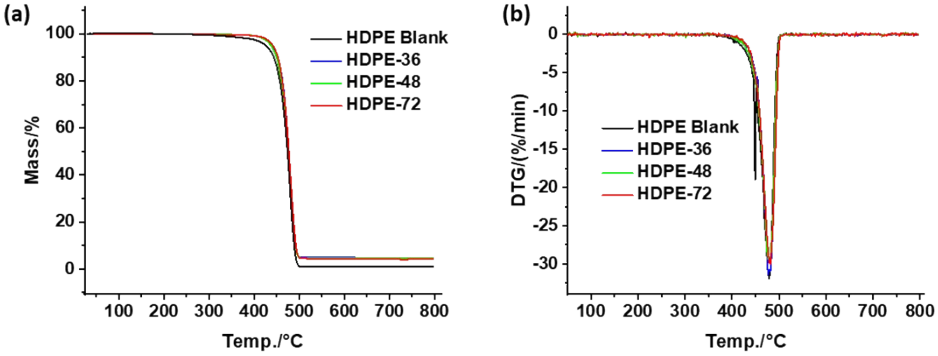

Fig. S7 *(a) TGA and (b) DTG curves of the untreated and treated HDPEs measured in N_2 environment.*

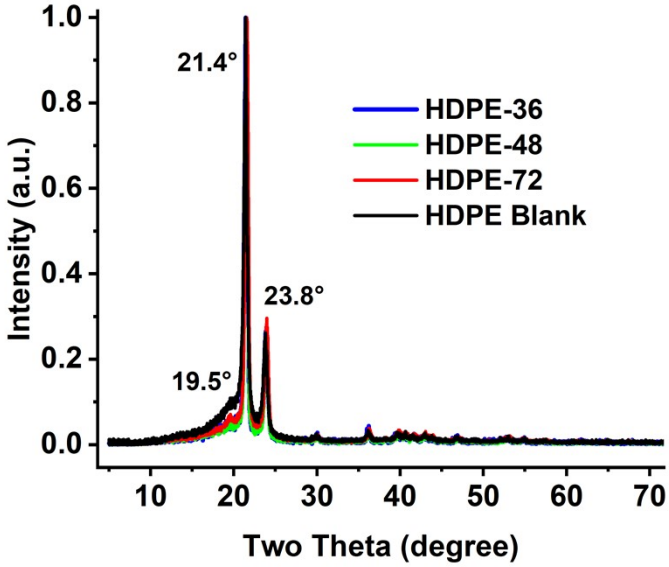

Fig. S8 *XRD patterns of HDPE Blank and treated HDPEs.*

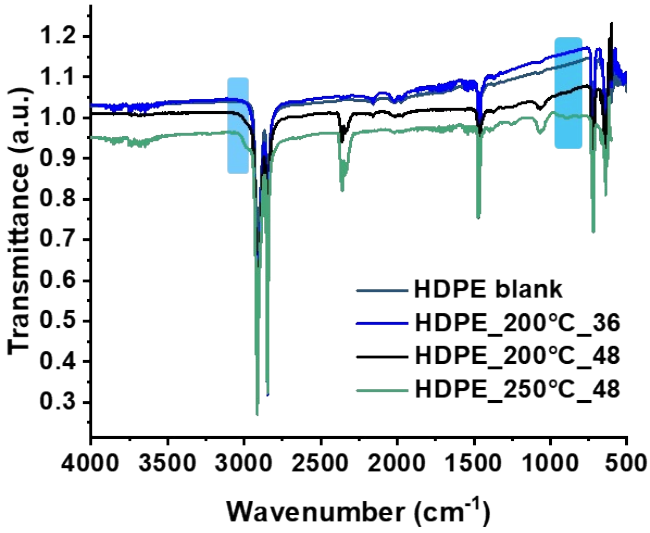

Fig. S9 *FTIR spectra of the HDPE before (blank) and after dehydrogenation treatment at 200 °C for 36 or 48 hours, in comparison with the HDPE-48 treated under 250 °C for 48 hours.*

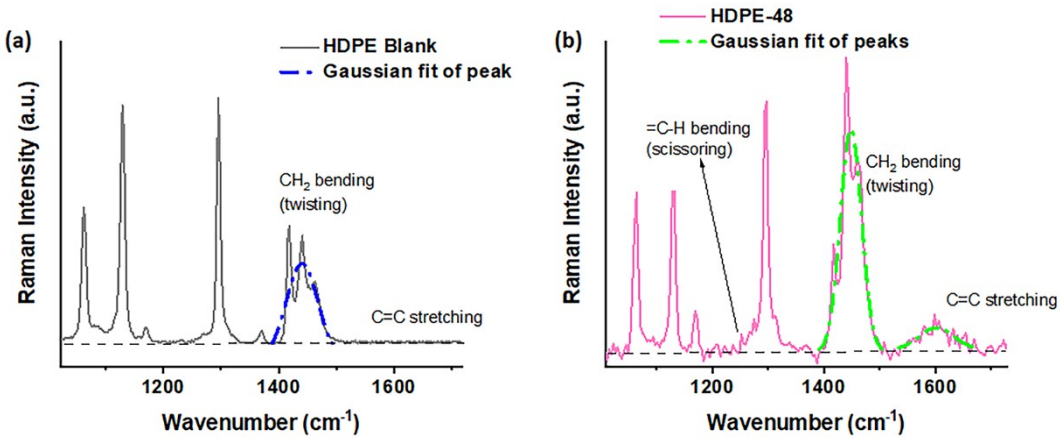

Fig. S10 *Gauss fitting and integration for evaluating band areas of (a) HDPE Blank, and (b) HDPE-48.*

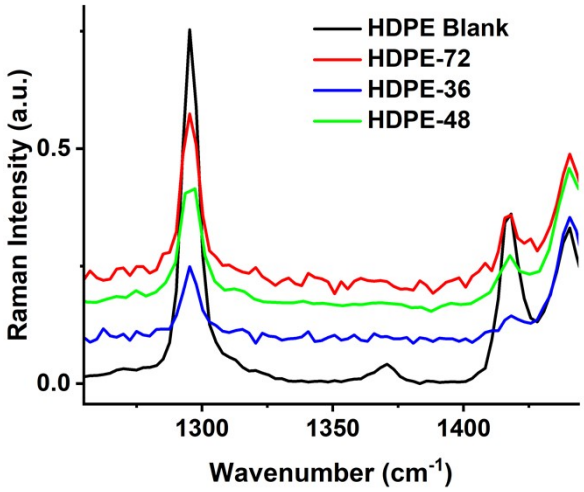

Fig. S11 *Raman spectra of the HDPEs before and after dehydrogenation treatment with enlarged area between 1250 – 1450 cm^{-1}.*

Table S2*. Degree of crystallinity (Xc) change for the dehydrogenated HDPEs calculated using the Strobl and Hagedorn method.*

Sample	X_c	Changes of X_c
HDPE Blank	0.58	0
HDPE-36	0.64	10%
HDPE-48	0.60	3%
HDPE-72	0.62	7%

Table S3*: Determination of the carbon sp^2 and sp^3 content in HDPE and treated HDPE using the component fitting of the XPS C1s photoelectron peak as well as from the determination of the D parameter corresponding to the width of the X-ray excited C KLL Auger peak.*

Sample	sp^2 [%] (from C 1s fitting)[a]	*D* parameter [eV][b]	sp^2 [%] (from *D* parameter)[b]
HDPE	2.7	13.1 ± 0.1	0
HDPE-72	11.8 ± 7.0	14.0 ± 0.2	17.3 ± 5.8

[a] The error is estimated from the fitting routine of the two components lying close together.

[b] The errors represent one standard deviation in the average of two measurements at different positions on the sample.

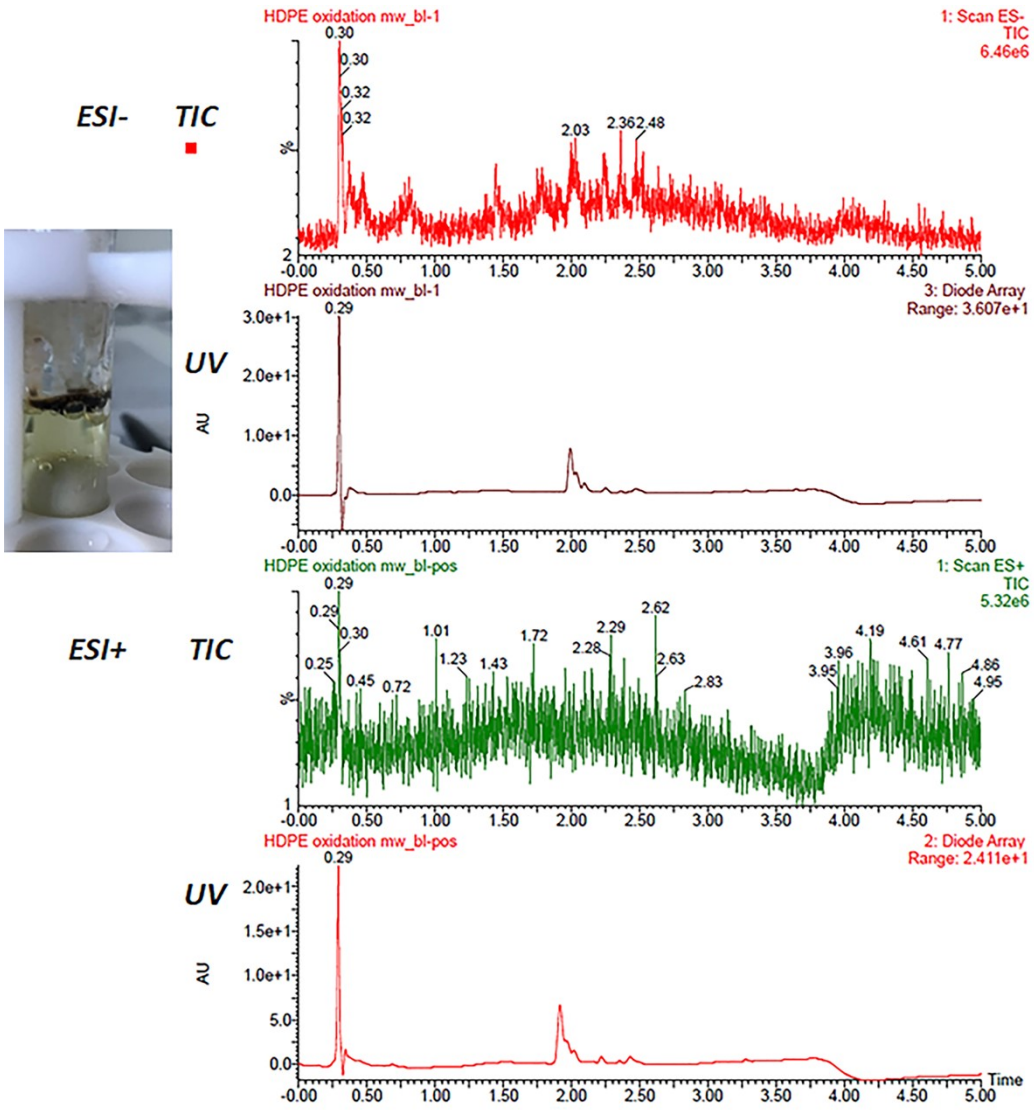

Fig. S12 *The oxidation solution of HDPE Blank (left), the UPLC-MS TIC and UV signals of the oxidation solution diluted in water (right), in (top) negative mode and (down) positive mode.*

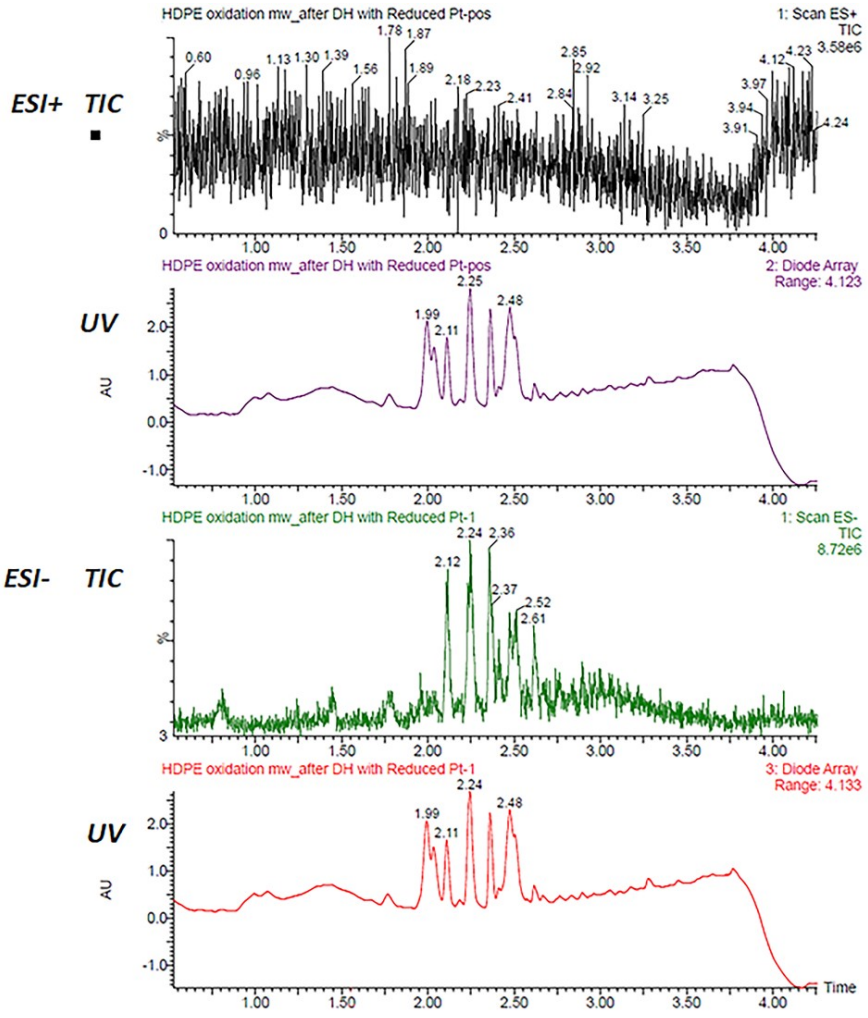

Fig. S13 *The UPLC-MS results of treated HDPE-48, with the TIC and UV signals of the oxidation solution diluted in water, in (top) negative mode and (down) positive mode.*

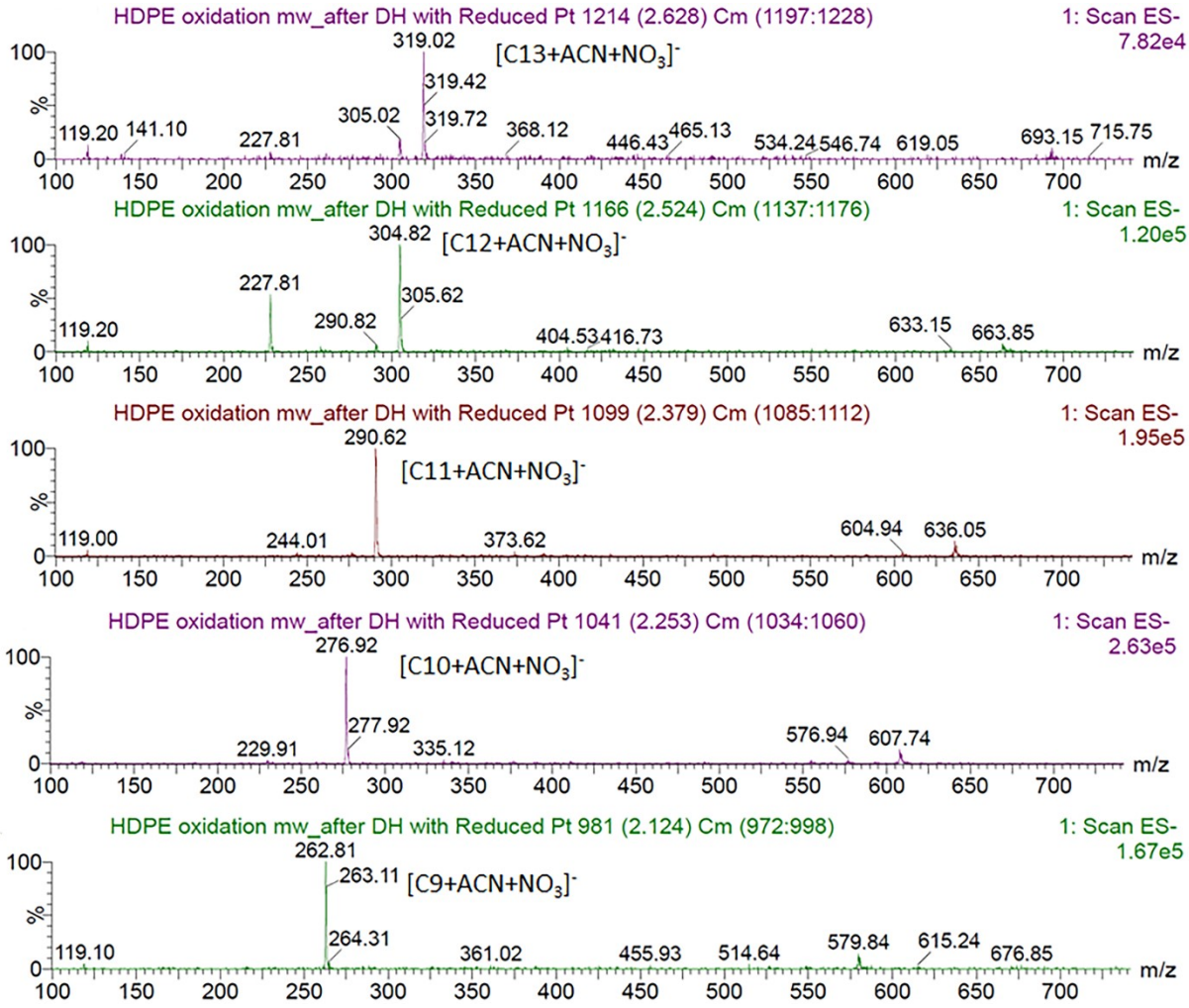

Fig. S14 *The extracted ion chromatograms measured by UPLC-MS of depolymerized products at different flow time. Data are corresponding to formic acid adducts of diacid species. Intensities are normalized to 100% for the highest peak in each chromatogram.*

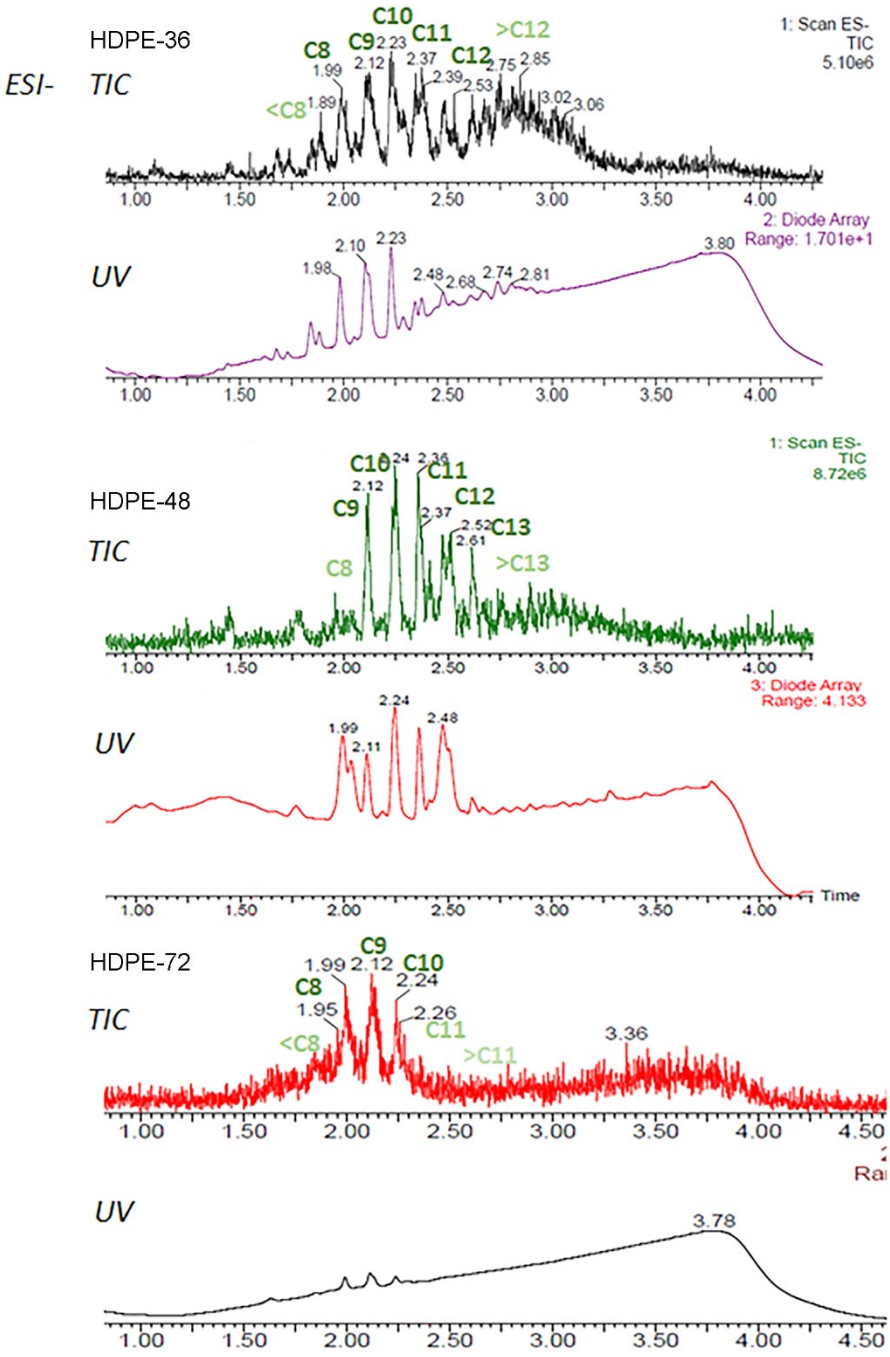

Fig. S15 *The UPLC-MS signals of the HDPE-36, HDPE-48, and HDPE-72 oxidation solution diluted in water characterized in TIC and UV channels, measured under ESI negative mode.*

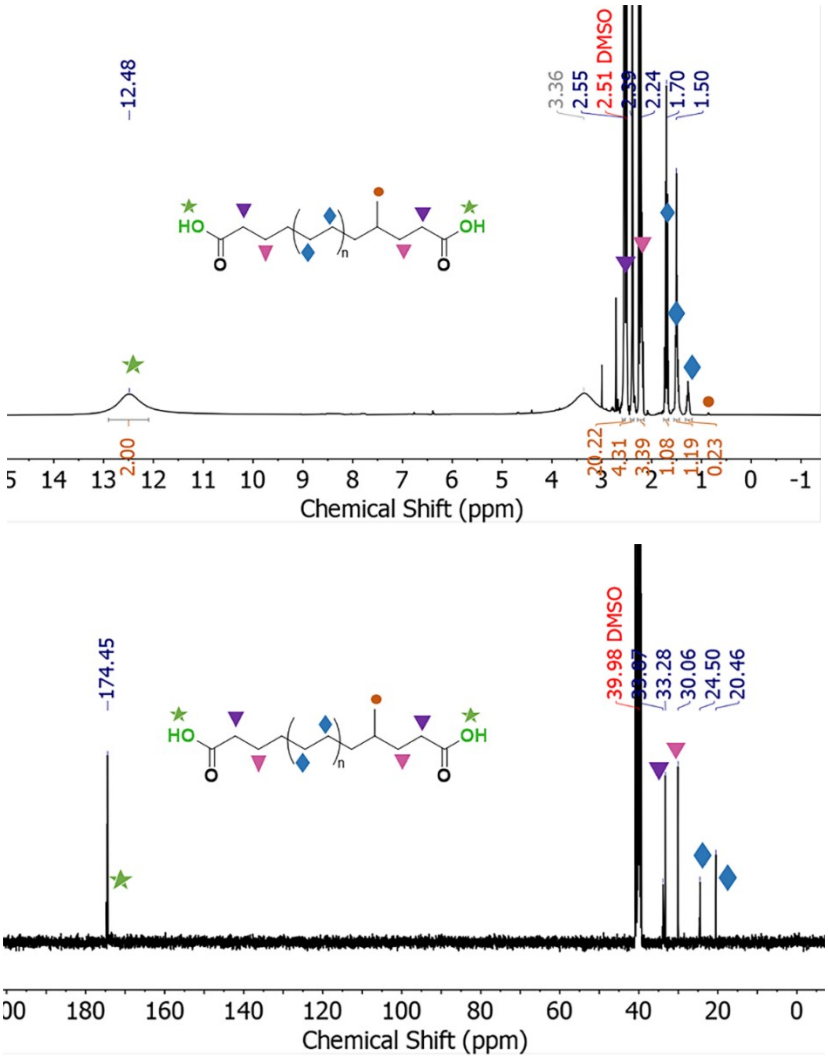

Fig. S16 *^{1}H (up) and ^{13}C (below) NMR spectra of the isolated oxidation products measured in DMSO-D_6.*

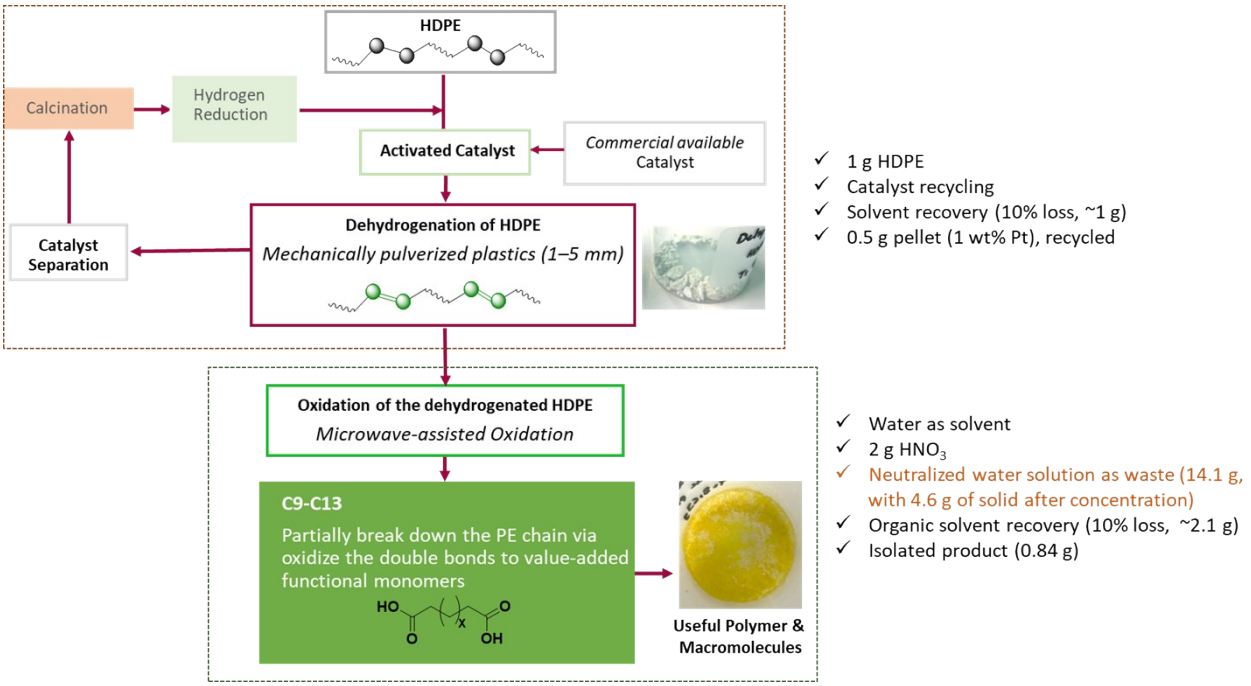

Fig. S17. *Waste generation during the two-step process of dehydrogenation and oxidation.*

Table S4*. E-Factors and sEF in synthesis of multi-functional molecules.*

Examples	Raw material	E-factor	sEF	Industry Sector
n-butanal [20]	Propylene	0.1	-	Bulk chemicals
Triphenols [21]	Vanillin, phenol	10.2	3.14	Fine chemicals
Atorvastatin [22]	Halohydrins, enzyme	18	5.8	Fine chemicals
Pregabalin [23]	2-carboxyethyl-3-cyano-5-methylhexanoic acid ethyl ester, lipolase	17	-	Fine chemicals
This work	HDPE waste	9.2	3.17	Fine chemicals

Table S5*. Molecular weights determined by GPC analysis of the oligomer and polyester after polycondensation, and their thermal properties measured by DSC.*

Peaks	M_n (g/mol)	M_w (g/mol)	PD (M_w/M_n)	T_m (°C)*	T_c (°C)*	ΔH_m (J/g)*
Oligomer	1639	5714	3.49	64	43	108
Polyester	2946	10401	3.53	73	60	143

* T_m and melting enthalpies (ΔH_m) measured by the DSC first heating up, T_c measured during cooling down, with heating/cooling rate of 10 °C/min.

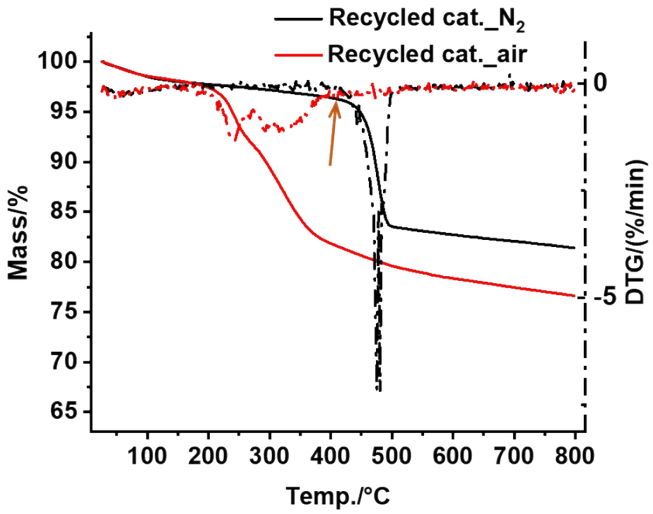

Fig. S18. *TGA and DTG (dashed) curves of the recovered catalyst before regeneration, measured in both air and N_2 environment.*

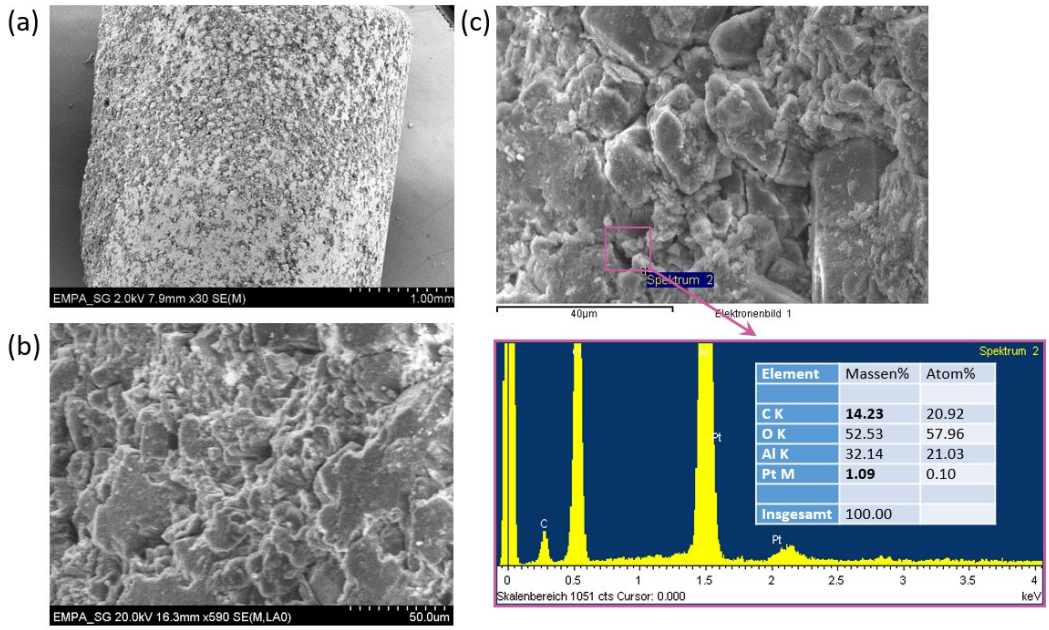

Fig. S19 *SEM and EDX of the recycled catalyst after one dehydrogenation use, (a) and (b) the surface morphology at different scales, and (c) EDX spectrum at a selected range with semi-quantitative amount of the elements.*

Literatures for supporting information

1. P. Rupper, M. Amberg, D. Hegemann and M. Heuberger, *Applied Surface Science*, 2020, **509**, 145362.
2. L.-S. Johansson, J. M. Campbell and O. J. Rojas, *Surface and Interface Analysis*, 2020, **52**, 1134-1138.

3. J. F. Moulder, W. F. Stickle, P. E. Sobol and K. D. Bomben, *Handbook of X-Ray Photoelectron Spectroscopy*, Perkin-Elmer Corporation, Physical Electronics Division, 1992.
4. S. Turgeon and R. W. Paynter, *Thin Solid Films*, 2001, **394**, 43-47.
5. B. Lesiak, J. Zemek, J. Houdkova, P. Jiricek and A. Jóźwik, *Polymer Degradation and Stability*, 2009, **94**, 1714-1721.
6. X. Jia and Z. Huang, *Nat Chem*, 2016, **8**, 157-161.
7. S. Chen, X. Chang, G. Sun, T. Zhang, Y. Xu, Y. Wang, C. Pei and J. Gong, *Chemical Society Reviews*, 2021, **50**, 3315-3354.
8. A. Arroyave, S. Cui, J. C. Lopez, A. L. Kocen, A. M. LaPointe, M. Delferro and G. W. Coates, *Journal of the American Chemical Society*, 2022, **144**, 23280-23285.
9. S. Avithi Kanniappan and U. B. R. Ragula, *Catalysts*, 2020, **10**.
10. X. Jie, S. Gonzalez-Cortes, T. Xiao, J. Wang, B. Yao, D. R. Slocombe, H. A. Al-Megren, J. R. Dilworth, J. M. Thomas and P. P. Edwards, *Angew Chem Int Ed Engl*, 2017, **56**, 10170-10173.
11. J. Choi, A. H. R. MacArthur, M. Brookhart and A. S. Goldman, *Chemical Reviews*, 2011, **111**, 1761-1779.
12. W. Y. Wu, A. M. Kirillov, X. H. Yan, P. P. Zhou, W. S. Liu and Y. Tang, *Angewandte Chemie-International Edition*, 2014, **53**, 10649-10653.
13. C. Li and G. Wang, *Chemical Society Reviews*, 2021, **50**, 4359-4381.
14. A. Ray, K. Zhu, Y. V. Kissin, A. E. Cherian, G. W. Coates and A. S. Goldman, *Chem Commun (Camb)*, 2005, DOI: 10.1039/b502120k, 3388-3390.
15. E. Bäckström, K. Odelius and M. Hakkarainen, *ACS Sustainable Chemistry & Engineering*, 2019, **7**, 11004-11013.
16. S. Ghatge, Y. Yang, J.-H. Ahn and H.-G. Hur, *Applied Biological Chemistry*, 2020, **63**, 27.
17. L. Genovese, M. Gigli, N. Lotti, M. Gazzano, V. Siracusa, A. Munari and M. Dalla Rosa, *Industrial & Engineering Chemistry Research*, 2014, **53**, 10965-10973.
18. B. Ellis, *Journal*, 2000.
19. G. R. Strobl and W. Hagedorn, *Journal of Polymer Science: Polymer Physics Edition*, 1978, **16**, 1181-1193.
20. A. Behr, M. Urschey and V. A. Brehme, *Green Chemistry*, 2003, **5**, 198-204.
21. S. Zhao and M. M. Abu-Omar, *Macromolecules*, 2017, **50**, 3573-3581.
22. R. J. Fox, S. C. Davis, E. C. Mundorff, L. M. Newman, V. Gavrilovic, S. K. Ma, L. M. Chung, C. Ching, S. Tam, S. Muley, J. Grate, J. Gruber, J. C. Whitman, R. A. Sheldon and G. W. Huisman, *Nature Biotechnology*, 2007, **25**, 338-344.
23. C. A. Martinez, S. Hu, Y. Dumond, J. Tao, P. Kelleher and L. Tully, *Organic Process Research & Development*, 2008, **12**, 392-398.